LETTER

doi:10.1038/nature12419

An observational correlation between stellar brightness variations and surface gravity

Fabienne A. Bastien[1], Keivan G. Stassun[1,2], Gibor Basri[3] & Joshua Pepper[1,4]

Surface gravity is a basic stellar property, but it is difficult to measure accurately, with typical uncertainties of 25 to 50 per cent if measured spectroscopically[1,2] and 90 to 150 per cent if measured photometrically[3]. Asteroseismology measures gravity with an uncertainty of about 2 per cent but is restricted to relatively small samples of bright stars, most of which are giants[4–6]. The availability of high-precision measurements of brightness variations for more than 150,000 stars[7,8] provides an opportunity to investigate whether the variations can be used to determine surface gravities. The Fourier power of granulation on a star's surface correlates physically with surface gravity[9,10]: if brightness variations on timescales of hours arise from granulation[11], then such variations should correlate with surface gravity. Here we report an analysis of archival data that reveals an observational correlation between surface gravity and root mean squared brightness variations on timescales of less than eight hours for stars with temperatures of 4,500 to 6,750 kelvin, log surface gravities of 2.5 to 4.5 (cgs units) and overall brightness variations of less than three parts per thousand. A straightforward observation of optical brightness variations therefore allows a determination of the surface gravity with a precision of better than 25 per cent for inactive Sun-like stars at main-sequence to giant stages of evolution.

Brightness variations of Sun-like stars are driven by many factors, including granulation[12], oscillations[11], rotation and magnetic activity[13]. As they evolve from high-surface-gravity (high-g) dwarfs to low-g giants, their convective zones deepen, they rotate more slowly, their magnetic activity diminishes, and their oscillation and granulation timescales increase, all of which change the nature of the brightness variations. It has been previously demonstrated that the power in granulation (as traced by the Fourier spectrum of the brightness variations) is inversely proportional to ν_{max}, the peak frequency of Sun-like acoustic oscillations[9,12]. Given that ν_{max} is itself proportional to g (ref. 11), it follows that g should manifest in brightness variations on timescales that trace granulation. Although physically we expect this, it is not immediately apparent that brightness variations can be used as an effective determinant of g because other phenomena not directly related to g—most importantly spots, plage and other sources of brightness variations driven by the star's magnetic activity—probably dominate the observed brightness variations. It is therefore necessary to filter out the brightness variations arising from these phenomena, which occur on timescales of hours to days, while preserving the brightness variations related to granulation and g on timescales of minutes to hours.

Using long-cadence (30 min) light curves from Quarter 9 of NASA's Kepler Mission[14], and representing them using the Filtergraph data visualization tool[15], we observe clear patterns in the evolutionary properties of stars encoded in three simple measures of their brightness variations[8] (Fig. 1): range (R_{var}), number of zero crossings (X_0), and root mean square on timescales shorter than 8 h (to which we will refer as '8-hr flicker' or F_8). Relating these measures to g determined asteroseismically from a sample of Kepler stars[4], we find distinctive features that highlight the way stars evolve in this three-dimensional space, making up an evolutionary diagram of photometric variability. Within this diagram, we find a vertical cloud of points, largely made up of high-g dwarfs, that have large R_{var}, small X_0 and low F_8 values. We observe a tight sequence of stars—a 'flicker-floor' sequence that defines a prominently protruding lower envelope in R_{var}—spanning gravities from dwarfs to giants. Sun-like stars of all evolutionary states evidently move onto this sequence only when they have a large X_0, which in turn implies low stellar activity.

We find that g is encoded in F_8, yielding a tight correlation between the two (Fig. 2). Moreover, using 11 yr of SOHO Virgo[16,17] light curves of the Sun and sampling them at the same cadence as the Kepler long-cadence light curves, we find that the Sun's (constant) g is also measurable using F_8, which remains invariant throughout the 11-yr solar activity cycle even while the Sun's R_{var} and X_0 values change considerably from the spot-dominated solar maximum to the nearly spotless solar minimum (Fig. 1). From the Sun's behaviour, we infer that a large portion of the Kepler stars' vertical scatter within the vertical cloud at the left of the diagram (Fig. 1) may be driven by solar-type cyclic activity variations. Most importantly, the Sun's true g fits our empirical relation (Fig. 2), and the g value of any Sun-like Kepler star from dwarf to giant may be inferred from this relation with an accuracy of 0.06–0.10 dex (Supplementary Information).

Asteroseismic analyses derive g from the properties of stellar acoustic oscillations[4,18–20]. Given that near-surface convection drives both these oscillations and granulation, and given the brightness variability timescales to which F_8 is sensitive, we suggest that a combination of different types of granulation (with typical solar timescales ranging from ~30 min to ~30 h; ref. 21) drives the manifestation of g in this metric. The precise timescales of these phenomena in solar-type stars depend strongly on the stellar evolutionary state and, hence, also on g (refs 5,9,10,22). Acoustic oscillations, whose amplitudes are sensitive to g (ref. 5), may provide an increasingly important contribution to F_8 as stars evolve into subgiants and giants and the amplitudes and timescales of these oscillations increase[5,9,10]. At some point, the pressure-mode and granulation timescales cross[9], which may lead to a breakdown of our F_8–g relation at very low values of g.

By using F_8 to measure g, we can construct a photometric variability evolutionary diagram for most stars observed by Kepler, even for stars well beyond the reach of asteroseismic and spectroscopic analysis (Fig. 3). By coding this diagram according to stellar temperature and rotation period, we may trace the physical evolution of Sun-like stars as follows: stars begin as main-sequence dwarfs with large photometric R_{var} values and small X_0 values, presumably driven by simple rotational modulation of spots at relatively short rotation periods. As the stars spin down to longer rotation periods, their brightness variations first become steadily 'quieter' (systematically lower R_{var}) but then become suddenly and substantially more complex (larger X_0) as they reach the flicker floor. Some stars reach the floor only after beginning their evolution as low-g subgiants, having moved to the right (higher F_8) as their effective temperatures begin rapidly dropping. Other stars

[1]Department of Physics and Astronomy, Vanderbilt University, 1807 Station B, Nashville, Tennessee 37235, USA. [2]Physics Department, Fisk University, 1000 17th Avenue North, Nashville, Tennessee 37208, USA. [3]Astronomy Department, University of California, Hearst Field Annex, Berkeley, California 94720, USA. [4]Physics Department, Lehigh University, 27 Memorial Drive West, Bethlehem, Pennsylvania 18015, USA.

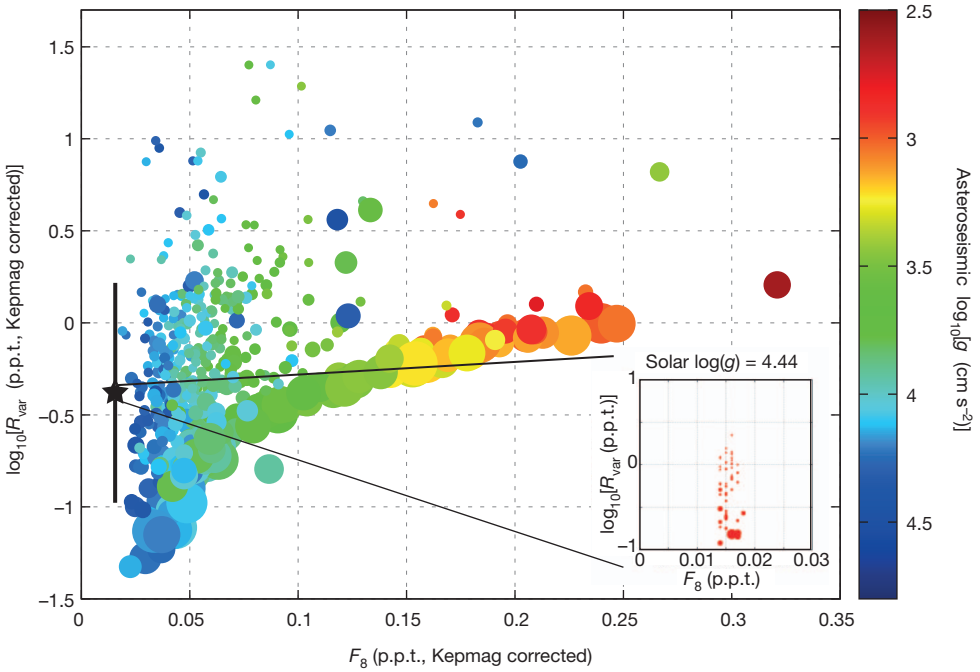

Figure 1 | Simple measures of brightness variations reveal a fundamental 'flicker sequence' of stellar evolution. We establish the evolutionary states of stars with three simple measures of brightness variations[8]. The abscissa, 8-h flicker (F_8), measures brightness variations on time scales of 8 h or less. The ordinate, R_{var}, yields the largest amplitude of the photometric variations in a 90-d timeframe. The number of zero crossings, X_0 (symbol size; ranging from 0.01 to 2.1 crossings per day), conveys the large-scale complexity of the light curve. We correct both R_{var} and F_8 for their dependence on Kepler magnitude (Kepmag). Colour represents asteroseismically determined g. We observe two populations of stars: a vertical cloud composed of high-g dwarfs and some subgiants, and a tight sequence—the flicker floor—spanning a range of g from dwarfs to giants. The typically large R_{var} values of stars in the cloud, coupled with their simpler light curves (small X_0), implies brightness variations driven by rotational modulation of spots. In contrast, large X_0 values characterize stars on the sequence. The F_8 values of stars in this sequence increase inversely with g because the physical source of F_8 is sensitive to g. R_{var} also increases with F_8 along the floor, because F_8 is a primary contributor to R_{var} (as opposed to starspots above the floor). Stars with a given F_8 value cannot have R_{var} less than that implied by F_8 itself: quiet stars accumulate on the flicker floor because they are prevented from going below it by the statistical definition of the two quantities. Stars above the floor have larger amplitude variations on longer timescales that set R_{var}. The large star symbol with vertical bars and the inset show the Sun's behaviour over the course of its 11-yr magnetic cycle. The Sun's F_8 value is largely invariant over the course of its cycle, just as its g value is invariant. p.p.t., parts per thousand.

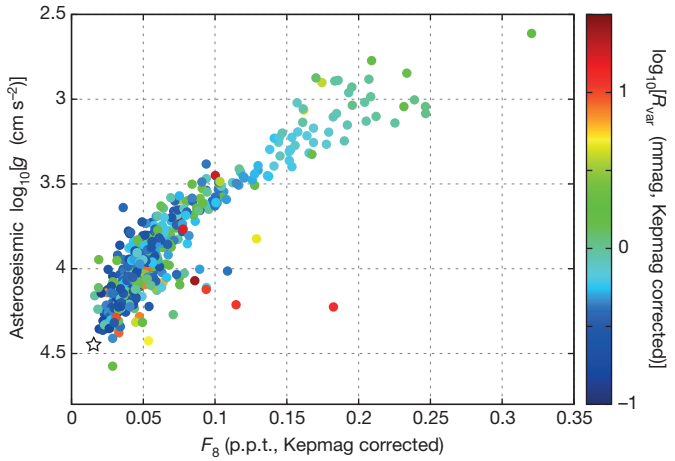

Figure 2 | Stellar surface gravity manifests in a simple measure of brightness variations. The same stars from Fig. 1 with Kepler Quarter 9 data. Asteroseismically determined[4] g shows a tight correlation with F_8. Colour represents the R_{var} of the stars' brightness variations; outliers tend to have large brightness variations. Excluding these outliers, a cubic-polynomial fit through the Kepler stars and through the Sun (large star symbol) shows a median absolute deviation of 0.06 dex and a root mean squared deviation of 0.10 dex (Supplementary Information). To simulate how the solar g would appear in the archival data we use to measure g for other stars, we divide the solar data into 90-d 'quarters'. Our F_8–g relation measured over multiple quarters then yields a median solar g of 4.442 with a median absolute deviation of 0.005 dex and a root mean squared error of 0.009 dex (the true solar g is 4.438).

join the sequence while still dwarfs; these are easily identified in our diagram by their drastically increased X_0 values at very low F_8. Evidently some dwarf stars become magnetically quiet while still firmly on the main sequence, whereas others do not reach the floor until they begin to swell considerably. We note that the Sun seems to approach the flicker floor at solar minimum; its R_{var} value becomes quite low and its X_0 value strongly increases (Fig. 1).

A star's main-sequence mass and initial spin probably determine where along the flicker-floor sequence it ultimately arrives, because the slope of a star's trajectory in our diagram is essentially determined by the ratio of its spin-down timescale (downward motion) and structural evolutionary timescale (rightward motion). Regardless, once on the floor all stars evolve along this sequence and stay on it as they move up to the red-giant branch, their effective temperatures steadily dropping as their surfaces rapidly expand. Despite their very slow rotation as subgiants and giants on the flicker-floor sequence, their photometric R_{var} is steadily driven upwards by the increasing F_8, which reflects the stars' continually decreasing g. The increasing R_{var} and F_8 values of subgiants and giants on the flicker floor is probably the result of the increasingly important contribution of radial and non-radial pulsations to the overall brightness variations[23,24].

A few stars appear as outliers to the basic picture we have presented here; these are seen towards the right of the vertical cloud of points in our evolutionary diagram (Fig. 3). Some active dwarfs have higher F_8 values than expected for their g values. Frequent strong flares can boost F_8 as currently defined, and some hotter dwarfs are pulsators with enough power near 8 h to increase their F_8 values. A few such cases appear also in the asteroseismic sample (Fig. 1). Some lower-g stars have R_{var} values above the flicker floor owing to the presence of magnetic

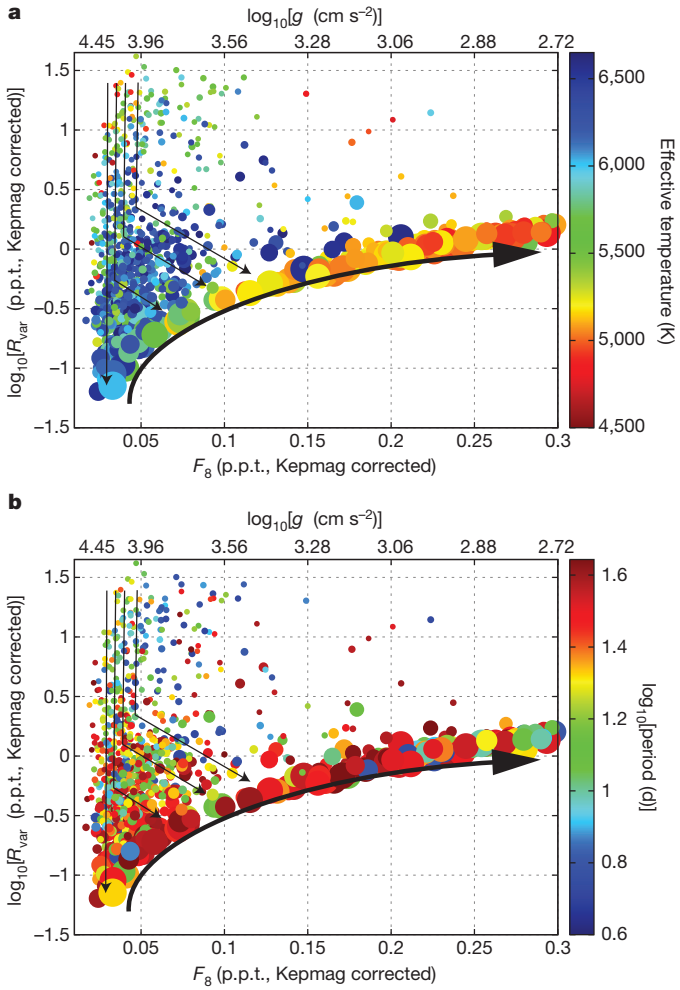

Figure 3 | An integrative view of stellar evolution in a new diagram of brightness variations. Same as Fig. 1, but for Kepler stars lacking asteroseismic *g*. We include a *g* scale at the top (from conversion of the F_8 scale at bottom via our calibrated relationship). Here we selected stars with Kepler magnitudes between 11.0 and 11.85 to limit the sample to ~1,000 stars for visual clarity (1,012 points are shown). We removed objects that are potentially blended (Kepler flux contamination greater than 0.05) as well as those that may be galaxies (Kepler star/galaxy flag other than 0). Arrows schematically indicate the evolutionary paths of Sun-like stars in this diagram. Stars generally move from top to bottom, as the overall brightness fluctuations due to spots decrease with time, and then from left to right as their *g* values decrease. All stars eventually arrive on the flicker-floor sequence and evolve along it. **a**, Colour represents effective temperature. Stars cool as they evolve from left to right, from dwarfs to red giants. We restricted the effective temperatures to be 4,500–6,650 K, using the revised temperature scale for Kepler stars[30]. **b**, Same as **a**, but colour-coded by the dominant periodicity in the light curve. We limited the sample to stars with dominant periods longer than 3 d (to eliminate very rapidly rotating active stars) and shorter than 45 d (half the Kepler 90-d data interval). This period traces rotation for unevolved stars and pulsations for evolved ones. Dwarfs generally show the expected spin-down sequence with decreasing R_{var} (correlated with the level of surface magnetic activity). Subgiants and giants broadly display very slow rotation, as expected.

activity[25], slow radial pulsations or secular drifts. Finally, a few outliers are simply due to data anomalies. As our technique is refined, these exceptions should be treated carefully before assigning a F_8-based *g* value, particularly for high-F_8 stars for which R_{var} is greater than ~3 parts per thousand. They constitute a small fraction of the bulk sample, and most of them can be identified as one of the above cases.

Common to all of the stars along the flicker floor is the virtual absence of spot activity as compared with their higher-R_{var} counterparts; short-timescale phenomena such as granulation and oscillations dominate the brightness variations. Given that spots probably suppress acoustic oscillations in the Sun and other dwarf stars[5,26–28], the large X_0 values of stars along this sequence may partly reflect the ability of short-timescale processes to manifest more strongly now that large spots no longer impede them, along with the increasing complexity of the convective variations. As the stars evolve into full-fledged red giants and beyond, the principal periodicity in their brightness variations increasingly reflects shorter-period oscillations, as opposed to their inherently long-period rotation, because oscillations become dominant over magnetic spots.

It may be possible to differentiate between stars with similar *g* values but different internal structures (for example first-ascent red giants versus helium-burning giants) through application of a sliding timescale of F_8 as a function of *g*, where the sliding timescale would capture the changing physical granulation timescales with evolutionary state[20]. Moreover, the behaviour of stars on the flicker floor may explain the source of radial velocity 'jitter' that now hampers planet detection through radial velocity measurements[29].

Received 2 April; accepted 20 June 2013.

1. Valenti, J. & Fischer, D. A. Spectroscopic properties of cool stars (SPOCS). I. 1040 F, G, and K dwarfs from Keck, Lick, and AAT planet search programs. *Astrophys. J.* **159,** 141–166 (2005).
2. Ghezzi, L. *et al.* Stellar parameters and metallicities of stars hosting Jovian and Neptunian mass planets: a possible dependence of planetary mass on metallicity. *Astrophys. J.* **720,** 1290–1302 (2010).
3. Brown, T. M., Latham, D. W., Everett, M. E. & Esquerto, G. A. Kepler Input Catalog: photometric calibration and stellar classification. *Astron. J.* **142,** 112–129 (2011).
4. Chaplin, W. J. *et al.* Ensemble asteroseismology of solar-type stars with the NASA Kepler mission. *Science* **332,** 213–216 (2011).
5. Huber, D. *et al.* Testing scaling relations for solar-like oscillations from the main sequence to red giants using Kepler data. *Astrophys. J.* **743,** 143–152 (2011).
6. Stello, D. *et al.* Asteroseismic classification of stellar populations among 13,000 red giants observed by Kepler. *Astrophys. J.* **765,** L41–L45 (2013).
7. Basri, G. *et al.* Photometric variability in Kepler target stars: the Sun among stars – a first look. *Astrophys. J.* **713,** L155–L159 (2010).
8. Basri, G. *et al.* Photometric variability in Kepler target stars. II. An overview of amplitude, periodicity, and rotation in the First Quarter data. *Astron. J.* **141,** 20–27 (2011).
9. Mathur, S. *et al.* Granulation in red giants: observations by the Kepler mission and three-dimensional convection simulations. *Astrophys. J.* **741,** 119–130 (2011).
10. Kjeldsen, H. & Bedding, T. R. Amplitudes of solar-like oscillations: a new scaling relation. *Astron. Astrophys.* **529,** L8–L11 (2011).
11. Brown, T. M., Gilliland, R. L., Noyes, R. W. & Ramsey, L. W. Detection of possible p-mode oscillations on Procyon. *Astrophys. J.* **368,** 599–609 (1991).
12. Gilliland, R. L. *et al.* Kepler mission stellar and instrument noise properties. *Astrophys. J.* **197** (suppl.), 6–24 (2011).
13. Strassmeier, K. G. Starspots. *Astron. Astrophys. Rev.* **17,** 251–308 (2009).
14. Borucki, W. J. *et al.* Kepler planet-detection mission: introduction and first results. *Science* **327,** 977–980 (2010).
15. Burger, D. *et al.* An interactive web application for visualization of astronomy datasets. *Astron. Comput.* (in the press); preprint at http://arxiv.org/abs/1307.4000 (2013).
16. Fröhlich, C. *et al.* First results from VIRGO, the experiment for helioseismology and solar irradiance monitoring on SOHO. *Sol. Phys.* **170,** 1–25 (1997).
17. Basri, G., Walkowicz, L. M. & Reiners, A. Comparison of Kepler photometric variability with the Sun on different timescales. *Astrophys. J.* **769,** 37–49 (2013).
18. Brown, T. M. & Gilliland, R. L. Asteroseismology. *Annu. Rev. Astron. Astrophys.* **32,** 37–82 (1994).
19. Christensen-Dalsgaard, J. Physics of solar-like oscillations. *Sol. Phys.* **220,** 137–168 (2004).
20. Chaplin, W. J. & Miglio, A. Asteroseismology of solar-type and red giant stars. *Annu. Rev. Astron. Astrophys.* (in the press).
21. Dumusque, X., Udry, S., Lovis, C., Santos, N. C. & Monteiro, M. J. P. F. G. Planetary detection limits taking into account stellar noise. I. Observational strategies to reduce stellar oscillation and granulation effects. *Astron. Astrophys.* **525,** 140–151 (2011).
22. Kjeldsen, H. & Bedding, T. R. Amplitudes of stellar oscillations: the implications for asteroseismology. *Astron. Astrophys.* **293,** 87–106 (1995).
23. Henry, G. W., Fekel, F. C., Henry, S. M. & Hall, D. S. Photometric variability in a sample of 187 G and K giants. *Astrophys. J.* **130** (suppl.), 201–225 (2000).
24. Gilliland, R. L. Photometric oscillations of low-luminosity red giant stars. *Astron. J.* **136,** 566–579 (2008).
25. Schröder, C., Reiners, A. & Schmitt, J. H. M. M. Ca II HK emission in rapidly rotating stars. Evidence for an onset of the solar-type dynamo. *Astron. Astrophys.* **493,** 1099–1107 (2009).
26. Chaplin, W. J., Elsworth, Y., Isaak, G. R., Miller, B. A. & New, R. Variations in the excitation and damping of low-l solar p modes over the solar activity cycle. *Mon. Not. R. Astron. Soc.* **313,** 32–42 (2000).

27. Komm, R. W., Howe, R. & Hill, F. Solar-cycle changes in GONG p-mode widths and amplitudes 1995–1998. *Astrophys. J.* **531,** 1094–1108 (2000).
28. Chaplin, W. J. *et al.* Evidence for the impact of stellar activity on the detectability of solar-like oscillations observed by Kepler. *Astrophys. J.* **732,** L5–L10 (2011).
29. Bastien, F. A. *et al.* Radial velocity variations of photometrically quiet, chromospherically inactive Kepler stars: a link between RV jitter and photometric flicker. *Astron. J.* (submitted).
30. Pinsonneault, M. *et al.* A revised effective temperature scale for the Kepler Input Catalog. *Astrophys. J.* **199** (suppl.), 30–51 (2012).

Supplementary Information is available in the online version of the paper.

Acknowledgements The research described in this paper makes use of Filtergraph (http://filtergraph.vanderbilt.edu), an online data visualization tool developed at Vanderbilt University through the Vanderbilt Initiative in Data-intensive Astrophysics. We acknowledge discussions with P. Cargile, K. Carpenter, W. Chaplin, D. Huber, M. Paegert, M. Sinha and D. Weintraub. We thank D. Huber and T. Metcalfe for sharing the average asteroseismic parameters of Kepler stars with us. F.A.B. acknowledges support from a NASA Harriet Jenkins Fellowship and a Vanderbilt Provost Graduate Fellowship. F.A.B. and K.G.S. acknowledge NSF PAARE grant AST-0849736.

Author Contributions F.A.B. and K.G.S. contributed equally to the identification and analysis of the major correlations. F.A.B. principally wrote the first version of the manuscript. K.G.S. prepared the figures. G.B. calculated the variability statistics of the Kepler light curves and performed an independent check of the analysis. J.P. checked against biases in the datasets. All authors contributed to the interpretation of the results and to the final manuscript.

Author Information Reprints and permissions information is available at www.nature.com/reprints. The authors declare no competing financial interests. Readers are welcome to comment on the online version of the paper. Correspondence and requests for materials should be addressed to F.A.B. (fabienne.a.bastien@vanderbilt.edu).